npj | climate and atmospheric science

www.nature.com/npjclimatsci

ARTICLE OPEN

Check for updates

Aerosol effects on the vertical structure of precipitation in East China

Nan Sun[1], Yunfei Fu[1]✉, Lei Zhong[1] and Rui Li[1]

In this paper, we examine the aerosol effects on the vertical structure of precipitation in East China by matching GPM DPR (Global Precipitation Measurement Dual-frequency Precipitation Radar) and MERRA-2 (Modern-Era Retrospective analysis for Research and Applications, Versions2) datasets. It was found that the increase of aerosol will obviously increase the precipitation frequency when AOD (Aerosol Optical Depth) ≤ 0.5, but the excessive aerosol suppresses the precipitation frequency when AOD > 0.5 in some regions. The AOD obviously enhances the radar echo intensity of precipitation and has a stronger impact on convective precipitation. The correlation between AOD and rain rate, and that between AOD and STH (storm top height) are different in different regions of East China. The aerosol reduces the mean droplet concentration in most regions except NC (Northeast China). In most cases, aerosol increases the effective radius of precipitation and has a higher impact on convective precipitation.

npj Climate and Atmospheric Science (2022)5:60 ; https://doi.org/10.1038/s41612-022-00284-0

INTRODUCTION

Aerosols, the key components of the atmosphere produced by both natural processes and anthropogenic activities, impinge on Earth's climate and hydrological cycle by altering the radiative balance of the atmosphere and precipitation formation[1–3]. IPCC[4] divided aerosols effects into the aerosol–radiation interaction (ARI) and the aerosol–cloud interaction (ACI), which describe how aerosols affect the scattering and absorption of radiation and cloud properties, respectively[5–7]. The different influence degrees of aerosols are reflected in the changes of various meteorological parameters, especially the changes in basic meteorological elements, such as temperature and precipitation[8–13].

The effects of aerosols on precipitation are essential but poorly understood, and many scholars have carried out a series of studies about that[14–17]. Aerosols affect precipitation through ARI and ACI processes[18]. Rosenfeld et al.[7] found that aerosols can both decrease and increase rainfall as a result of their radiative and cloud condensation nuclei (CCN) activities. Li et al.[3] further show that precipitation frequency and rain rate are altered by aerosols. They observed that rain increases with aerosol in deep clouds that have a high liquid-water content, but declines in clouds that have a low liquid-water content. Koren et al.[19] pointed out that the turning zone exists in the influence of aerosols on clouds and precipitation. Using TRMM PR precipitation datasets along with MODIS Aerosols products, Dong et al.[17] studied the potential impacts of Sahara dust on the rainfall vertical structure and found that dust aerosols can raise the storm height of stratiform rain significantly.

East China is one of the fastest developing regions in China. Since the reform and opening up in the late 1970s, the concentrations of sulfuric acid, carbonaceous and mineral dust aerosols have increased obviously in China[13], especially in East China. A large number of aerosols will reduce air quality, change atmospheric physical and chemical properties, and then affect weather and climate. In recent years, the East China has experienced a frequency of continuous and severe haze pollution, catching extensive concern of scholars[20–26]. Using MERRA-2 dataset, Xu[26] presented the long-term variations of surface and column black carbon over East China. Using 3 years of 3-hourly observations made in heavily polluted eastern China, Jiang et al.[18] concluded that rainfall amounts from deep convective clouds increased at first and then decreased as aerosol optical depth increased. Guo et al.[27] found that China is above this zone with an increasing aerosol trend, and the United States is below it with a decreasing trend, but they have similar reductions in local-scale precipitation (LSP) hours. While many studies have revealed the effect of aerosol on precipitation over China, few have studied the aerosol effects on the vertical and microphysical structure of precipitation in East China. To fully understand the effects, accurate microphysical parameters with high vertical resolution are required. Historically, most three-dimensional precipitation data since 1997 are from Tropical Rainfall Measuring Mission Precipitation Radar (TRMM PR)[28–32]. However, microphysical precipitation parameters are not available in TRMM PR. Airborne Radar and Ground Based Radar can provide microphysical data about precipitation but the method is challenging and costly, and it is also difficult to obtain data in real time. Besides, ground-based radar cannot serve this role because ground radar's vertical resolution is poor at the far range.

In addition to high vertical resolution precipitation data, the acquisition of aerosol data near the precipitation events is also one of the difficulties for study. The main characteristics of aerosol pollution are complex components, large transmission range, and widely distributed in the vertical direction. In the past, field sampling at fixed stations and ground-based remote sensing could not meet the requirements of accurate research and tracking of aerosol pollution. Satellite remote sensing can make up for this deficiency. At present, scholars used to study aerosols by passive remote sensing (such as Moderate-resolution Imaging Spectroradiometer, MODIS) to obtain global aerosol information. It is important to note that MODIS has inversion only in the cloudless area under a clear sky, and observation is made in the same area only once a day. Therefore, there will be very large amounts of missing measurements of aerosols on cloudy and rainy days, which means that MODIS cannot detect the aerosol content near the precipitation events, and it is difficult to

[1]School of Earth and Space Sciences, University of Science and Technology of China, Hefei, China. ✉email: fyf@ustc.edu.cn

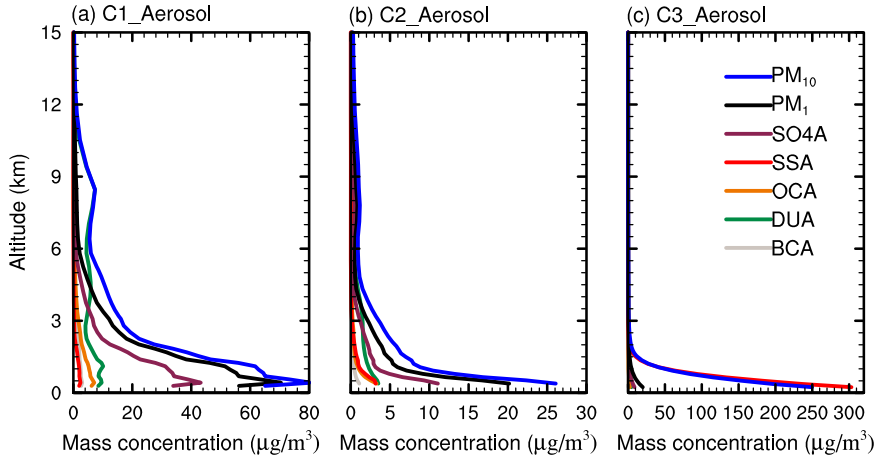

Fig. 1 Aerosol mass concentration profile of cases. a Case1 (C1). **b** Case 2 (C2). **c** Case 3 (C3).

accurately study the relationship between aerosol and precipitation by passive remote sensing. Besides, passive remote sensing has high retrieval uncertainty in high albedo areas, and cannot detect aerosol with high vertical resolution information. The active remote sensing satellites can make up for the shortcomings of passive remote sensing satellites. For example, launched on April 28, 2006, CALIPSO (Cloud-Aerosol Lidar Infrared Pathfinder Satellite Observations) carry CALIOP (Cloud-Aerosol Lidar with Orthogonal Polarization), which has realized the continuous observations of the three-dimensional distribution characteristics of global aerosols during the day and night for the first time. However, CALIPSO still has the problems of low temporal resolution (revisit cycle of 16 days) and small spatial coverage. Considering that the time and location of precipitation events are random, if the precipitation data are matched with CALIPSO, the sample size will be too small to accurately study the relationship between pollution and precipitation.

In recent years, the state-of-the-art Dual-frequency Precipitation Radar (DPR) carried by Global Precipitation Measurement (GPM) along with the latest generation of reanalysis datasets MEERRA-2 (Modern-Era Retrospective Analysis for Research and Applications, version 2) have provided new insight into the aerosol effects on the vertical and microphysical structure of precipitation.

GPM launched in February 2014, carrying the first spaceborne dual frequency rain measurement radar DPR. Designed jointly by JAXA (Japan Aerospace Exploration Agency) and NICT (National Institute of Communication Technology), DPR contains two bands of precipitation radar, namely KuPR (Ku band, 13.6 GHz) and KaPR (Ka band, 35.5 GHz). Based on the different echo characteristics of Ku band and Ka band, the dual channel inversion algorithm can be used to retrieve DSD (Droplet Size Distribution), which provides excellent opportunities for studying the microphysical structure of precipitation. In addition, the accuracy of DSD has also been verified[33].

MERRA-2 is released in 2017 by the NASA Global Modeling and Assimilation Office (GMAO)[34]. MERRA-2 provides data since 1980 and is the first long-term global reanalysis to assimilate space-based observations of aerosols and represent their interactions with other physical processes in the climate system. Based on the Goddard Earth Observing System Model Version 5 (GEOS-5), the MERRA-2 assimilation system uses AOD (Aerosol Optical Depth) measurements from the Advanced Very-High-Resolution Radiometer (AVHRR), ground-based Aerosol Robotic Network (AERONET), the Multiangle Imaging SpectroRadiometer (MISR), and the Moderate Resolution Imaging Spectroradiometer (MODIS). MERRA-2 provides high spatiotemporal resolution AOD data, which attracts many scholars' interest and the reliability of the data is proved[26,34].

In this paper, we carry out three case analyses and conduct statistical analyses to study aerosol effects on precipitation by matching the precipitation profiles from GPM DPR with aerosol data from MERRA-2. In addition, the climatological characteristics of aerosol and precipitation over East China are analyzed.

RESULTS

Studying area

To understand the impact of aerosol on precipitation in different areas, we divide East China into three regions according to its climate characteristics and previous studies[35] (Supplementary Fig. 1). From north to south, they are NC (Northeast China; 38°–50°N, 118°–130°E), MEC (Middle and East China; 26.5°–38°N, 112°–123°E), and SC (South China; 18°–26.5°N, 108°–123°E).

Case study

To have a preliminary understanding and lay a foundation for statistical analysis, we analyze three cases selected from NC, MEC, and SC, respectively (Supplementary Fig. 2). The DPR is matched with MERRA-2 and the matching time is 1 h. The flow field is superimposed over the plot. In addition, to observe the distribution of AOD before and after rainfall, the AOD and wind field 6 and 3 h before and 3 h after rainfall are also analyzed. Case 1 occurs in NC (Supplementary Fig. 2c) and the atmosphere near the precipitation is polluted seriously. Most precipitation occurs in polluted area. We can see that the pollution of precipitation area 6 h before precipitation is serious. With the passage of time, the pollution increase gradually and the pollution tends to reduce 3 h after precipitation. Case 2 occurs in MEC (Supplementary Fig. 2j). The precipitation in the north of 32°N mainly occurs in the "Dirty' area. In the south of 32°N, with 31°N and 118°E as the center, the precipitation in the 1°grid around is mainly "Clean," and the surrounding precipitation is mainly slightly polluted. Before and after precipitation, the precipitation area is mainly slightly polluted. Case 3 occurs in SC (Supplementary Fig. 2k), the precipitation region is mainly slightly polluted. On the left of the precipitation area, there is a heavily polluted area, and the pollution gradually reduced after the precipitation.

To study the vertical distribution of aerosol, we calculate the mass concentration profiles of SO4A (SO4 Aerosol), SSA (Sea Salt Aerosol), OCA (Organic Carbon Aerosol), DUA (Dust Aerosol), BCA (Black Carbon Aerosol), PM_1 (Particulate Matter 1), and PM_{10} (Particulate Matter 10) at the occurrence time of three cases, shown as Fig. 1. For case1, the aerosols distribute mostly below the altitude of 3 km and the aerosol concentration is the highest near the ground. The main aerosol in this precipitation event is

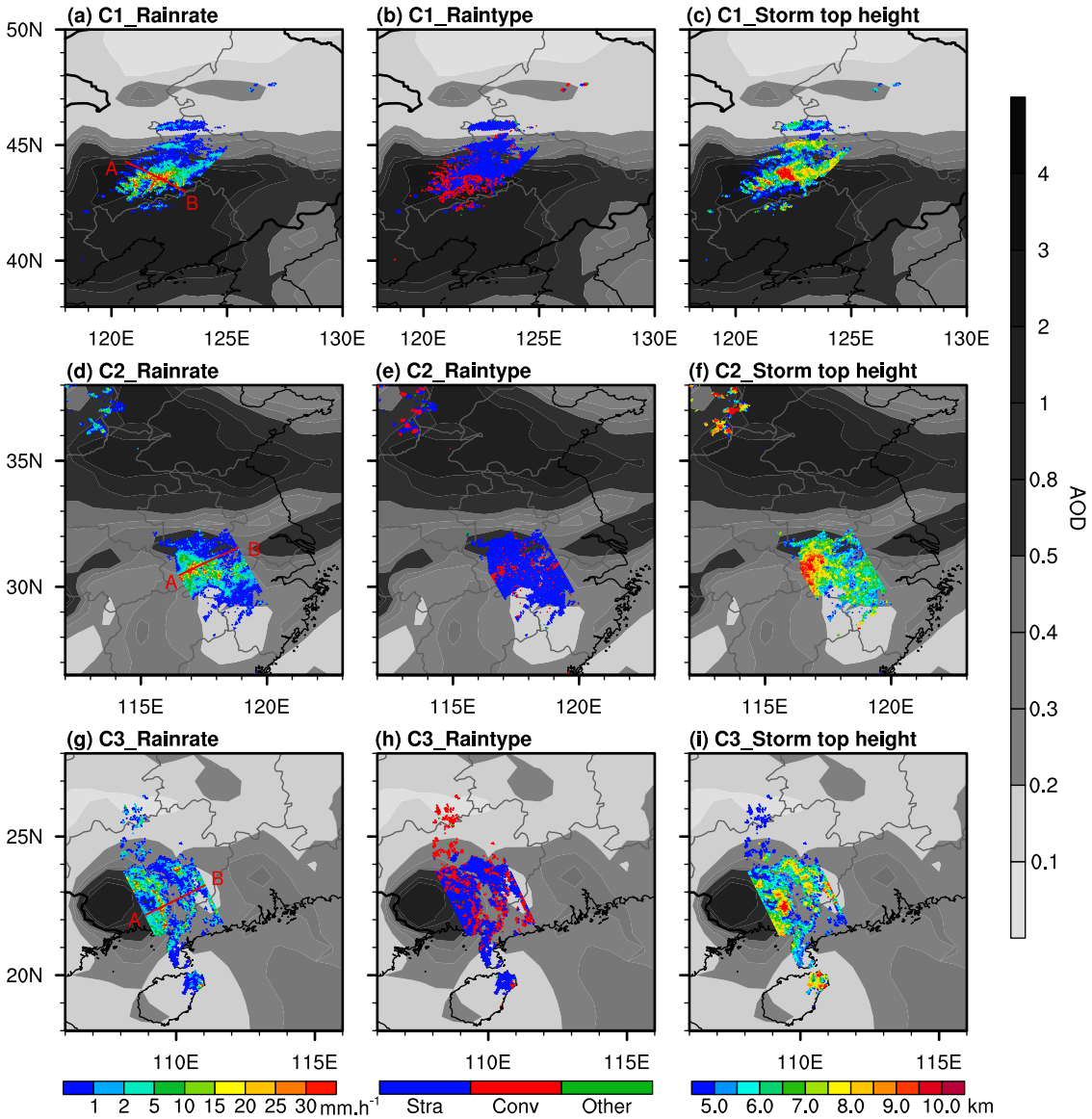

Fig. 2 Aerosol horizontal distribution cases. **a** Distribution of AOD and rain rate in C1. **b** Distribution of AOD and rain type in C1. **c** Distribution of AOD and storm top height in C1. **d** Distribution of AOD and rain rate in C2. **e** Distribution of AOD and rain type in C2. **f** Distribution of AOD and storm top height in C2. **g** Distribution of AOD and rain rate in C3. **h** Distribution of AOD and rain type in C3. **i** Distribution of AOD and storm top height in C3.

SO4A and its maximum value can reach 44 μg/m^3 at the altitude of 400 m. The mass concentration of the other four types of aerosols is no more than 10 μg/m^3. The maximum value of PM_1 and PM_{10} are also at 400 m altitude, and they are 71 and 80 μg/m^3, respectively. The profiles shape of SO4A, PM_1, and PM_{10} are similar, and all of them show that the concentration of SO4A, PM_1, and PM_{10} gradually increase from ground to 400 m, reaching the maximum at 400 m, and then gradually decreases above 400 m, which show that SO4A contributes mostly to the PM_1 and PM_{10}, and the proportion of PM_{10} is higher than that of PM_1. For case 2, the pollution degree of which is obviously less than that of case 1. The maximum concentration value of the five types of aerosol is no more than 11.2 μg/m^3. Similar to case 1, SO4A is also the main pollution in this precipitation event. Near the ground, the aerosol concentration is the highest, and the SO4A can reach 11.2 μg/m^3, the maximum of the other aerosol is no more than 4 μg/m^3, and the maximum of PM_1 and PM_{10} are 20.2 and 26.2 μg/m^3, respectively. The SO4A is still the main contributor to this precipitation event. The situation of case 3 is very different from that of case 1 and case 2. The aerosol of case 3 is concentrated mainly below 1.5 km. The aerosol concentration is the biggest near the ground, and SSA concentration is extremely high, up to 303 μg/m^3. The other types of aerosol concentration at the surface are no more than 9 μg/m^3. The maximum of PM_{10} and PM_1 are 250 and 20 μg/m^3, respectively, near surface and PM_1 is 12.5 times than PM_1, and the SSA is the major contributor to PM_{10}. Case 3 is actually the Super Typhoon Rammasun, which is the strongest storm landing in South China since 1973. The super typhoon landed in Guangxi Zhuang Autonomous Region and carried a large number of SSA, leading to the extremely high value of SSA of this precipitation event.

To study further, we analyze the rain rate, rain type, and STH (storm top height) in three cases, shown in Fig. 2. In case 1 (Fig. 2a–c), The high-value area of rain rate occurs in "Dirty" area and the maximum can reach to 30 mm/h, The low value distributes in the "Clean" and "Other" areas and the maximum does not exceed 5 mm/h. Furthermore, convective precipitation mainly occurs in the "Dirty" area, where the maximum STH can reach

10 km. Stratiform precipitation mainly occurs in "Clean" and "Other" areas and the STH is obviously lower than precipitation in "Dirty" area, most of which is no more than 8.5 km. In case 2 (Fig. 2d–f) heavy precipitation mainly occurs in the slightly polluted area ($0.2 \le AOD \le 0.5$) and the maximum can reach 30 mm/h. This precipitation is mainly stratiform precipitation and the maximum STH can reach to 10 km. In case 3 (Fig. 2g–i), precipitation occurs on the right of the "Dirty" area and heavy rain occurs on the "Dirty" area. This precipitation is a mixture of stratiform and convective precipitation and the maximum STH can reach 9.5 km.

The radar reflectivity cross sections along the line AB in Fig. 2a, d, g are shown in Supplementary Fig. 3. In case 1 (Supplementary Fig. 3a), the strong echo occurs at 250–300 km away from point A, with the strongest up to 50 dBZ. The strong echo appears at the height of 0-4 km, where the AOD is 2.5–3, belonging to the "Dirty" area. In case 2 (Supplementary Fig. 3b), the strong echo occurs at 80–110 km away from point A, the strongest echo here is 40–50 dBZ and the AOD here is 0.15–0.2, belonging to the "Clean" area. In case 3 (Supplementary Fig. 3c), the maximum echo occurs 110–130 km away from point A and the strongest echo is more than 45 dBZ. The STH here can reach 12 km and the AOD is 0.4–0.5, an "Other" area.

The average distribution of Black Carbon AOD (BCaod), Dust AOD (Daod), Organic Carbon AOD (OCaod), Sea Salt AOD (SSaod), Sulfate AOD (SO_4aod), and Total AOD (Taod) from 2014 to 2020 in summer are calculated, shown as Supplementary Fig. 4. In general, the aerosol content in MEC is highest and the AOD in most areas exceed 0.3, which belongs to "Clean" and "Other." The highest area of AOD is the junction of Shandong, Hebei, and Henan, with the highest AOD can reach to 0.7. Taking this area as the central point, the AOD gradually decreases towards the outer ring and the lowest area of AOD is in Northern Fujian, which is 0.3. More than half of MEC is located in the "Dirty" area. The AOD in NC is lower than that in MEC, and AOD in NC is 0.15-0.65. Most areas of NC belong to "Dirty" and "Other" areas. The most polluted area is located in the southwest corner of NC, which gradually decreases from southwest to northeast (Supplementary Fig. 4f). Among the five types of aerosol, the SO4aod is the highest and its AOD content and distribution are close to that of the Taod. The AOD of SO4aod is about 0.1 lower than that of Taod, and the AOD of SO4aod and Taod are about one order of magnitude higher than that of other types of aerosols. In NC, the second highest AOD is OCaod. From northeast to southwest, OCaod tends to decrease, ranging from 0.03 to 0.08. The third highest AOD is Daod, ranging from 0.02 to 0.05, which gradually decreases from west to east, because the dust aerosol mainly comes from the west. The lowest AOD in NC are BCaod (0.01–0.05) and SSaod (0–0.02). In MEC, the order of other AOD is OCaod (0.01–0.08), Daod (0–0.06), BCaod (0.01–0.06), and SSaod (0–0.04). In SC, on the whole, the AOD is lower than that in NC and MEC and the overall environment is cleaner. The second highest AOD are OCaod and SSaod, in which OCaod gradually decreases from north to south, with a maximum up to 0.05, SSaod mainly comes from the surrounding ocean, and the maximum is along the coast, with a maximum up to 0.06. The BCaod and Daod are the lowest, no more than 0.02.

To understand the precipitation in East China, we first calculate the total sample number and the sample number of stratiform and convective precipitation, shown in Supplementary Fig. 5. As we can see, the total sample number gradually decreases from north to south and the NC has the highest sample number, ranging from 21,500 to 25,000, followed by the MEC, with a maximum of 22,500, and the SC is the lowest, the maximum no more than 22,000. The stratiform sample number ranges from 200 to 2000 (Supplementary Fig. 5b). In general, the high-value area of stratiform precipitation sample number in SC is slightly less than that in MEC and NC. In NC, the sample number in the northeast is higher than that in the southwest and that in most parts of the northeast is more than 1200, while that in most parts of the southwest is between 600 and 1200. In MEC, the high value is distributed in the intersection areas of Hunan, Anhui, and Jiangxi, as well as Northern Zhejiang and Fujian. The sample number for most of these areas is more than 1200. In SC, the high-value areas appear in the south of Taiwan and the middle of Guangxi, and most of the samples of high-value areas exceed 1600. Taking 31°N as the dividing line, the convection samples in the south of East China are obviously higher than that in the north. Most of the samples in the north are no more than 400, and most of the samples in the south are more than 400. The maximum is in Guangxi, southern Guangdong, and southern Taiwan, up to 1200.

The precipitation frequency under "Dirty," "Other," and "Clean" conditions are calculated, shown in Supplementary Fig. 6. In general, the frequency under "Dirty" and "Other" conditions are obviously higher than that under "Clean" condition. Under the "Clean" condition, the frequency (1–7%) of SC, Inner Mongolia in NC, the northeast of Heilongjiang, and the east of Jilin, is obviously higher than the frequency (<1%) of MEC and the middle and southern NC. The highest frequency is in the Hainan, south of Taiwan, and the northernmost part of Inner Mongolia, up to 7%. Under "Dirty" condition, the frequency in the middle and south of MEC, and the south of the NC are the highest, where the frequency of most areas is more than 2%, with a maximum of up to 7%. The frequency (<1%) of the rest areas in East China is obviously lower than in these areas (Supplementary Fig. 6a–c). Under the "Other" condition, the frequency in the south MEC and SC, with the most area over 4%, is obviously higher than that in the rest area. The distribution of frequency for the stratiform precipitation under "Dirty," "Clean," and "Other" are similar to the "Total" situation, but the frequency of the high-value area is about 1% lower than the "Total" situation. The frequency of convective precipitation is obviously lower than that of stratiform precipitation. Under the "Clean" condition, the frequency of SC is relatively high and the highest frequency is in Hainan, which can reach 2%. Under the "Dirty" condition, the frequency in East China is relatively lower overall, no more than 3%, and the frequency of MEC is relatively higher, with most area up 1%. Under the "Other" condition, frequency in SC and south of MEC are the highest, with most areas more than 1%. The north of MEC and NC are the lowest, with a maximum of no more than 1%.

Aerosol effects on the vertical structure of precipitation

To further study the influence of aerosol on the vertical structure of precipitation, we calculate the rain rate profiles under "Clean," "Dirty," and "Other" conditions (Supplementary Fig. 7). In NC, the rain rate under "Clean" conditions is the lowest, while that under "Dirty" conditions is the highest, and rain rate under "Other" condition is between that under "Clean" and "Dirty" conditions. For stratiform rain rate, the differences in rain rate under three AOD conditions are the biggest below 5 km altitude. From the altitude of 1 to 3 km, the difference in rain rate between "Clean" and "Dirty" is about 0.3 mm/h. From 3 to 5 km, the difference gradually decreases. Above 5 km, their rain rate is almost the same. For convective rain rate, from 1 to 3 km, the max rain rate difference between "Clean" and "Dirty" can reach about 2.1 mm/h. Above 3 km, their difference gradually decreases, and there is almost no difference between them near 10 km. In MEC, For stratiform rain rate, the "Dirty" rain rate is lower than the "Clean" rain rate and aerosol suppress rain rate. From 1 to 5 km, the "Dirty" rain rate is 0.2–0.3 mm/h lower than the "Clean" rain rate. Above 5 km, their difference gradually decreases with altitude. There is almost no difference above 6 km. For convective rain rate, from 1 to 4 km, the "Dirty" rain rate is higher than the "Clean" rain rate and the biggest difference can reach 0.8 mm/h. Above 4 km, the "Dirty" rain rate is slightly lower than the "Clean" rain rate and their difference is no more than 0.2 mm/h. In SC, for stratiform rain rate, the differences between the three conditions are very small, with

the maximum no more than 0.1 mm/h. For convective rain rate, the performance in SC is consistent with other most situations and the "Dirty" rain rate is higher than the "Clean" rain rate. From 1 to 3 km, the difference between "Dirty" and "Clean" is about 0.7 mm/h. From 3 to 4.5 km, their difference gradually decreases to 0.2 mm/h and above 4.5 km their difference is about 0.2 mm/h.

In general, the influence of aerosol on the convective rain rate profiles is greater than that of stratiform, and aerosol has a greater influence on the rain rate profiles of NC and MEC. For convective precipitation, aerosol promotes rain rate, however, this is not the case for stratiform precipitation. For stratiform precipitation, the red lines in Supplementary Fig. 7 yield the highest rain rate in NC, lowest rain rate in MEC, and no difference in SC under 5 km altitude, which is mainly due to the different aerosol concentrations and aerosol types in different regions. More and smaller cloud droplets generate under high aerosol conditions, which can effectively inhibit the collision growth process, delay the formation of precipitation, and prolong and strengthen the condensation growth process of cloud droplets and produce additional cloud water yield. The above process, on the one hand, causes the convective precipitation with a strong updraft to carry more and smaller cloud droplets to higher altitudes to condense and release more latent heat, which can lead to the further strengthening of its vertical movement and the increase of its precipitation intensity, which explains why the aerosol obviously promote the rain rate of convective precipitation. On the other hand, for stratiform precipitation, the average value of AOD over more than half of MEC is greater than 0.5, which means that the pollution degree of most "Dirty" precipitation of MEC is obviously more serious than that of NC and SC. The excessive aerosol makes the additional cloud water produced by the cloud droplet condensation and growth process too high to be carried by the stratiform precipitation with the weak updraft so that its vertical movement is inhibited and the rain rate is also inhibited. The pollution degree of "Dirty" precipitation in NC is less serious than that of MEC. In this aerosol concentration range, the increased aerosol concentration will lead to more efficient condensation, more latent heat release, and more cloud water. In SC, SSA, SO4A, and OCA are the main components. For stratiform precipitation with the weak updraft, when SSA is included in the environment with SO4A and OCA, the SSA consumes a large amount of supersaturated water vapor and inhibits the activation of submicron aerosols[36], which explains why the aerosols have no effect on the "Dirty" stratiform precipitation in SC. However, for the convective precipitation with a strong updraft, the total number of activated sea salt particles increases significantly, resulting in an increase in the total number of activated particles[37], which increases the "Dirty" convective precipitation rate in SC.

Next we study the DPDH (the distribution of probability density with height) of stratiform radar reflectivity under three AOD conditions, shown in Supplementary Fig. 8. In general, the radar echo inside the rain mass between NC, MEC, and SC are different and that under different aerosol conditions are also different. The echo top height in NC is the lowest, ranging about 10 km. The high-value region of echo frequency (>0.1%) is mainly distributed between 0–6 km and 15–30 dBZ, and the frequency is basically greater than 0.12%. In NC, the maximum radar echo can reach 41 dBZ, and the maximum echo top height can reach 9.6 km under "Clean" condition. Compared with that, the radar echo under the "Dirty" condition is wider and higher, with maximum echo top height up to 10.3 km and maximum echo up to 42.1 dBZ. The frequency of high-value region of echo under the "Dirty" condition (>0.1%) is lower than that under the "Clean" condition (0.1%). Under the "Other" condition, the maximum echo top height can reach 10 km and the maximum echo is 40 dBZ. The echo top height in MEC is about 11 km, which is between NC and SC. The high-value region of echo frequency (>0.1%) distribute between 0–3.5 km and 15–18 dBZ, and between 2–6.5 km and 17–27 dBZ. The frequency between 0–3.5 km and 15–18 dBZ is above 0.12%, 0.01–0.02% higher than that between 2–6.5 km and 17–27 dBZ. The echo top height in SC is highest, about 11.5 km, and the maximum echo can reach about 40 dBZ.

The DPDH of convective radar reflectivity under three AOD conditions, shown in Supplementary Fig. 9. We can see that the radar echo structure between three regions is obviously different and the difference between radar echo under different aerosol conditions is also very obvious. The echo top height in NC is the lowest (~11 km) and the maximum echo is the strongest. The echo top height in MEC is about 12 km, higher than that in NC, and that in SC is the highest, about 12.5–13 km. The maximum echo in MEC is slightly higher than that in SC. In NC, the echo top height under the "Dirty" condition is the highest, about 11.6 km, and the maximum echo is the strongest. The echo top height under the "Clean" condition is the lowest (~11 km) and the maximum echo is the weakest. In MEC, the echo top height under the "Clean" condition is the highest, about 12.6 km, and the maximum echo is the weakest. The echo top height under the "Dirty" condition is about 12.1 km and the maximum echo is the strongest. In SC, the echo top height under the "Dirty" condition is the highest, about 13 km and the maximum echo is also the strongest. The echo top height under the "Clean" condition is the lowest, about 12.5 km and the echo is the weakest. In general, the maximum echo under the "Dirty" condition is always the strongest. The echo top height under the "Dirty" condition in NC and SC is the highest while that in MEC is not which indicates that aerosol does not necessarily make the echo top higher, but makes the maximum echo stronger for convective precipitation.

To understand the correlation between AOD and precipitation, we analyze the correlation between AOD and rain rate, AOD, and STH. In addition, the significance of these parameters under 95% confidence is tested, shown in Supplementary Fig. 10. Overall, the increase of AOD has an impact on the rain rate and STH, and there are both positive and negative correlations under some rain types in some regions. For stratiform, the correlation between AOD and rain rate in NC and MEC passes the significance test, but that in SC does not pass the test. AOD and rain rate in NC show a positive correlation, and the regression coefficient is 0.320 while there is a negative correlation between the two in MEC and the regression coefficient is −0.388 (Supplementary Fig. 10a). For convection, only the NC pass the test and neither the MEC nor SC pass the test. The regression coefficient in NC is 2.334 (Supplementary Fig. 10b).

Next, we analyze the correlation between AOD and STH (Supplementary Fig. 10c, d). For stratiform (Supplementary Fig. 10c), the NC and MEC pass the significance test while the SC does not pass the test. In NC, the STH increases with AOD, and the regression coefficient is 0.422, while in MEC, the STH decreases with AOD, and the regression coefficient is −0.523. For convection, the NC and SC pass the significance test, and AOD and STH show a positive correlation, with regression coefficients of 0.754 (NC) and 0.160 (SC). The MEC does not pass the test.

Aerosol effects on the microphysical structure of precipitation

To understand the influence of aerosol on the microphysical structure of precipitation, we conduct the profiles of dBN_0 and D_0 under "Clean," "Dirty," and "Other" conditions, shown as Figs. 3 and 4.

We first analyze profiles of D_0 (Fig. 3). In MEC and SC, the dBN_0 under the "Dirty" condition is obviously lower than that under the "Clean" condition. The dBN_0 under the "Other" condition is between that under the "Dirty" and "Clean" conditions overall. In NC, the dBN_0 of convective precipitation under "Dirty" is obviously higher than that under "Clean." In NC, for stratiform precipitation, at the altitude 1–4 km, the dBN_0 under "Dirty" is slightly higher than that under "Clean" and their difference is no more than 0.2. From 4 to 9.5 km, the dBN0 under "Dirty" is lower than that under

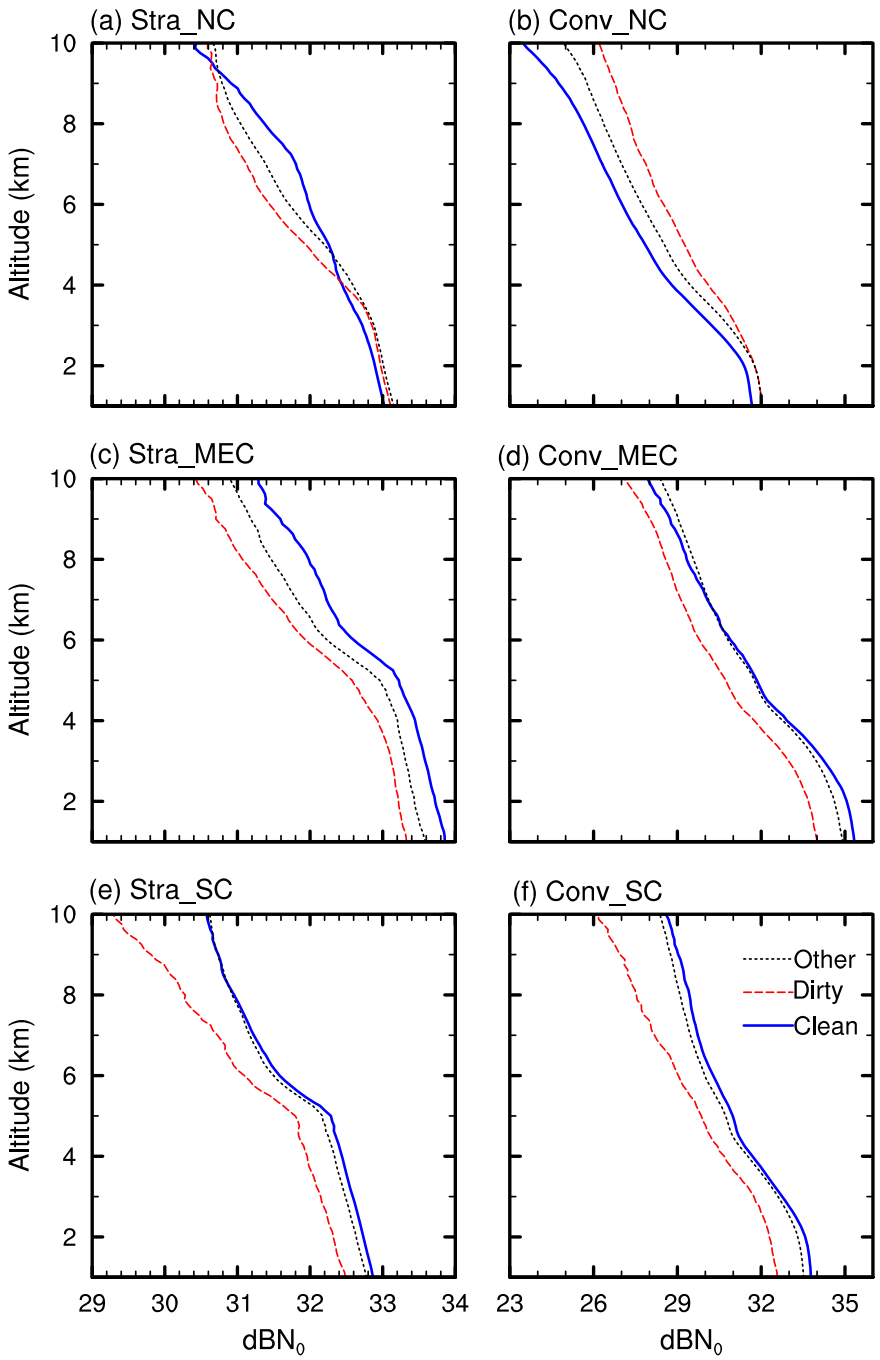

Fig. 3 The droplet concentration (dBN_0) profiles under "Clean," "Dirty," and "Other" conditions. **a** Stratiform precipitation in NC. **b** Convective precipitation in NC. **c** Stratiform precipitation in MEC. **d** Convective precipitation in MEC. **e** Stratiform precipitation in SC. **f** Convective precipitation in SC.

"Clean" and their difference first increases and then decreases with altitude. Their difference reaches the maximum (0.7) at ~7 km. For convective precipitation, From the surface to 10 km, the dBN_0 under "Dirty" is higher than that under "Clean" and their difference is minimum near the surface, no more than 0.4. Their difference increase with altitude and reaches the biggest (2.4) at 10 km. In MEC, the difference in stratiform precipitation between "Dirty" and "Clean" are 0.3–0.6 and that of convective precipitation is 0.2–0.9. The dBN_0 in SC is about 1–2 lower than that in MEC. For stratiform precipitation, the differences between "Dirty" and "Clean" are 0.1–0.3 and for convective precipitation, their differences are 0.5–1.5.

Next, we analyze profiles of D_0, shown in Fig. 4. On the whole, most regions show that the D_0 under "Dirty" is bigger than that under "Clean," while the D_0 under "Dirty" is less than that under "Clean" for stratiform precipitation in MEC and NC at some altitudes. Overall, the difference of D_0 between "Dirty" and "Clean" for convective precipitation is bigger than that for stratiform precipitation. In NC, D_0 of stratiform precipitation range from 1.13 to 1.31 mm. The maximum difference between "Dirty" and "Clean" is 0.05 mm. For convection, D_0 under "Dirty" is bigger than that under "Clean" from 0 to 5 km and their difference is biggest (0.08 mm) near the surface. As the height increases, their difference gradually decreases to 0 mm.

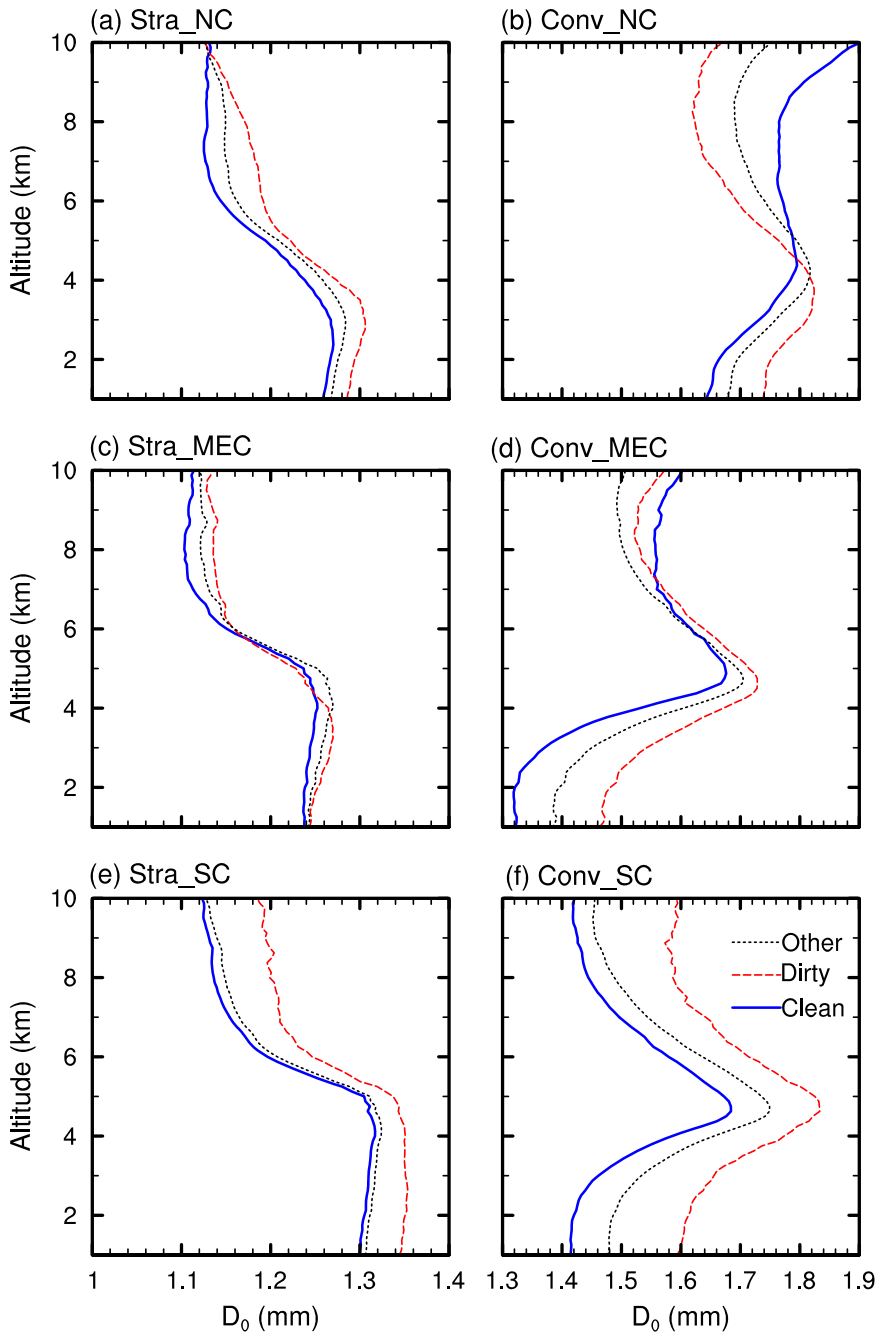

Fig. 4 The effective radius (D_0) profiles under "Clean," "Dirty," and "Other" conditions. a Stratiform precipitation in NC. **b** Convective precipitation in NC. **c** Stratiform precipitation in MEC. **d** Convective precipitation in MEC. **e** Stratiform precipitation in SC. **f** Convective precipitation in SC.

Above 5 km, D_0 under "Clean" is bigger than that under "Dirty" and their difference increase with altitude. At 10 km, the maximum difference is 0.22 mm. In MEC, the D_0 under "Dirty" is slightly bigger than that under "Clean" and their biggest difference is no more than 0.02 mm. For convection, from 1 to 7.4 km, the D_0 under "Dirty" is bigger than that under "Clean" and their biggest difference is near the surface. Their difference gradually decreases to 0 mm with the increase in altitude. Above 7.4 km, the D_0 under "Dirty" is lower than that under "Clean" and their biggest difference is no more than 0.05 mm. In SC, for stratiform, the difference of D_0 between "Dirty" and "Clean" is 0.02–0.03 mm and that for convection is 0.1–0.13 mm.

DISCUSSION

Aerosol effects on precipitation are essential but poorly understood caused by the lack of microphysical parameters for precipitation and the aerosol data with high spatiotemporal resolution. Based on the GPM DPR and the MERRA-2 data, we examine the impact of aerosol on the vertical and microphysical structure of precipitation over East China. The main conclusions are:

The AOD of MEC is the highest and that of SC is the lowest. Among the five types of aerosol, the SO4aod is the highest and that of most parts in East China is over 0.2, with maximum up to 0.7. The AOD of other four types of aerosols is no more than 0.1, which is about one order of magnitude lower than that of SO4aod.

Both NC and MEC are dominated by SO4aod, OCaod, and Daod, while SC is mainly SO4aod and SSaod.

The impacts of aerosol on precipitation frequency are different in different regions of East China. The increase of aerosol will obviously enhance the precipitation frequency when AOD ≤ 0.5, but the excessive aerosol suppresses the precipitation frequency in SC, the south of MEC, and the north of the NC when AOD > 0.5. However, in the rest parts of East China, the aerosol still increases precipitation frequency when AOD > 0.5.

Aerosol has an obvious effect on the rain rate. Aerosol increases rain rate obviously in most cases; however, Aerosol reduces rain rate in some cases. In NC and SC, Aerosol increases rain rate, and the enhancement effect of Aerosol on convective rain rate is greater than that of stratiform rain rate. In MEC, for the convection, from surface to 5 km, Aerosol still enhances the rain rate, but above 5 km, Aerosol suppresses the rain rate and Aerosol has an inhibitory effect on the stratiform rain rate.

The internal radar echo of precipitation in different regions of East China is obviously different. The Aerosol obviously enhances the radar echo intensity of precipitation and has a stronger impact on convective precipitation.

AOD and rain rate show a different correlation in different regions of East China. In NC, they show a positive correlation, and the correlation of convection is higher than that of stratiform. In MEC, for stratiform, AOD and rain rate show a negative correlation. However, there is no correlation between the stratiform and convection of SC and the convection of MEC. The correlation between AOD and STH is also different in different regions. In NC, they show a positive correlation and that of convection is higher than that of stratiform. For stratiform in MEC, they show a negative correlation, but for the convection, they do not pass the significance test. In SC, only convection passes the significance test, and the two show a positive correlation.

In most cases, when AOD > 0.5, aerosol reduce the mean droplet concentration, while aerosol increase the droplet concentration in a few cases. In MEC and SC, Aerosols obviously reduce the droplet concentration. In NC, from surface to 4 km, Aerosols slightly increase droplet concentration and above 4 km, Aerosols still reduce droplet concentration. For convection, Aerosols increase the droplet concentration obviously and the higher the altitude, the higher the Aerosols increase the droplet concentration.

Overall, Aerosols increase the effective radius and Aerosols have a higher impact on convection. In a few cases, Aerosols reduce the effective radius, for example, the convective precipitation above 5 km in NC and above 7.4 km in MEC.

The results of this study are expected to improve our understanding of the aerosol-precipitation interaction, lay a foundation for the follow-up study of the physical process, and provide more accurate precipitation profiles as the input of the model simulation. In the future, more precipitation microphysical parameters with the higher spatiotemporal resolution are expected.

METHODS

DPR-based precipitation dataset

GPM covers the world from 65°S to 65°N and the orbital period is 93 min. There are about 16 orbits around the earth every day. The DPR has a swath of 245 km and scans each time 49 pixels. The three-dimensional structure of precipitation from the surface to 22 km can be detected. Rainfall vertical structure datasets are collected from the GPM level 2 product 2ADPR in version 6 from 2014 to 2020 in summer (June, July, and August). The horizontal resolution is 5 km and the vertical resolution is 125 m. The DSD parameters provided by GPM 2ADPR include droplet concentration (dBN_0) and effective radius (D_0).

Merra-2-based AOD dataset

Here use the MERRA-2 aerosol assimilation product from 2014 to 2020 in summer. The time resolution is 1 h and the horizontal resolution is 0.5° × 0.625°. The six parameters provided by this dataset are used in this paper and they are Black Carbon AOD (BCaod), Dust AOD (Daod), Organic Carbon AOD (OCaod), Sea Salt AOD (SSaod), Sulfate AOD (SO_4aod), and Total AOD (Taod).

The classification basis for the aerosol

To learn about the impact of different aerosol content on precipitation, we divide the aerosol content into three categories according to our tests and the previous studies[13,17]. The three categories are "Clean (AOD < 0.2)," "Other (0.2 ≤ AOD ≤ 0.5)," and "Dirty (AOD > 0.5)."

DATA AVAILABILITY

MERRA-2 data are taken from https://disc.gsfc.nasa.gov/datasets?keywords=merra-2&page=1. GPM DPR data are archived at https://gpm.nasa.gov/data/directory.

CODE AVAILABILITY

The code developed to analyze the data of the study is available on request from the corresponding author.

Received: 16 December 2021; Accepted: 22 June 2022;
Published online: 25 July 2022

REFERENCES

1. Ramanathan, V., Crutzen, P. J., Kiehl, J. T. & Rosenfeld, D. Aerosols, climate, and the hydrological cycle. *Science* **294**, 2119–2124 (2001).
2. Feingold, G., Jiang, H. & Harrington, J. Y. On smoke suppression of clouds in Amazonia. *Geophys. Res. Lett.* **32**, L02804 (2005).
3. Li, Z. et al. Long-term impacts of aerosols on the vertical development of clouds and precipitation. *Nat. Geosci.* **4**, 888–894 (2011).
4. IPCC. *Climate Change 2013-The Physical Science Basis* (Intergovernmental Panel on Climate Change, 2013).
5. Ming, Y., Ramaswamy, V., Ginoux, P. A. & Horowitz, L. H. Direct radiative forcing of anthropogenic organic aerosol. *J. Geophys. Res. Atmos.* **110**, D20208 (2005).
6. Lohmann, U. et al. Total aerosol effect: radiative forcing or radiative flux perturbation. *Atmos. Chem. Phys.* **10**, 3235–3246 (2010).
7. Rosenfeld, D. et al. Flood or drought: how do aerosols affect precipitation. *Science* **321**, 1309–1313 (2008).
8. Menon, S., Del Genio, A. D., Koch, D. & Tselioudis, G. GCM simulations of the aerosol indirect effect: Sensitivity to cloud parameterization and aerosol burden. *J. Atmos. Sci.* **59**, 692–713 (2002).
9. Qian, Y. et al. Heavy pollution suppresses light rain in China: observations and modeling. *J. Geophys. Res. Atmos.* **114**, D00K02 (2009).
10. Li, Z. Q. et al. Aerosol and monsoon climate interactions over Asia. *Rev. Geophys.* **54**, 866–929 (2016).
11. Wu, G. X. et al. Advances in studying interactions between aerosols and monsoon in China. *Sci. China Earth Sci.* **59**, 1–16 (2016).
12. Li, Z. Q. et al. East Asian study of tropospheric aerosols and their impact on regional clouds, precipitation, and climate (EASTAIR CPC). *J. Geophys. Res. Atmos.* **124**, 13026–13054 (2019).
13. Li, Z. Q. Impact of aerosols on the weather, climate and environment of China: an overview (in Chinese). *Trans. Atmos. Sci.* **43**, 76–92 (2020).
14. Rosenfeld, D. et al. Inverse relations between amounts of air pollution and orographic precipitation. *Science* **315**, 1396–1398 (2007).
15. Lee, S. S., Guo, J. P. & Li, Z. Q. Delaying precipitation by air pollution over the Pearl River Delta: 2. Model simulations. *J. Geophys. Res. Atmos.* **121**, 11739–11760 (2016).
16. Jiang, M. J. et al. Potential influences of neglecting aerosol effects on the NCEP GFS precipitation forecast. *Atmos. Chem. Phys.* **17**, 13967–13982 (2017).
17. Dong, X., Li, R., Wang, Y., Fu, Y. & Zhao, C. Potential impacts of Sahara dust aerosol on rainfall vertical structure over the Atlantic Ocean as identified from EOF analysis. *J. Geophys. Res. Atmos.* **123**, 8850–8868 (2018).
18. Jiang, M., Li, Z., Wan, B. & Cribb, M. Impact of aerosols on precipitation from deep convective clouds in eastern China. *J. Geophys. Res. Atmos.* **121**, 9607–9620 (2016).
19. Koren, I. et al. Smoke invigoration versus inhibition of clouds over the Amazon. *Science* **321**, 946–949 (2008).

20. Luo, Y. F. et al. Characteristics of the spatial distribution and yearly variation of aerosol optical depth over China in last 30 years. *J. Geophys. Res. Atmos.* **106**, 14501–14513 (2001).
21. Qin, Y. & Xie, S. Spatial and temporal variation of anthropogenic black carbon emissions in China for the period 1980–2009. *Atmos. Chem. Phys.* **12**, 4825–4841 (2012).
22. Ding, A. et al. Intense atmospheric pollution modifies weather: a case of mixed biomass burning with fossil fuel combustion pollution in eastern China. *Atmos. Chem. Phys.* **13**, 10545–10554 (2013).
23. Ding, A. et al. Enhanced haze pollution by black carbon in megacities in China. *Geophys. Res. Lett.* **43**, 2873–2879 (2016).
24. Parrish, D. D. & Zhu, T. Clean air for megacities. *Science* **326**, 674–675 (2009).
25. Zhang, R. et al. Formation of urban fine particulate matter. *Chem. Rev.* **115**, 3803–3855 (2015).
26. Xu, X. et al. Characteristics of MERRA-2 black carbon variation in East China during 2000–2016. *Atmos. Environ.* **222**, 117140 (2020).
27. Guo, J. P. et al. Declining summertime local-scale precipitation frequency over China and the United States, 1981—2012: the disparate roles of aerosols. *Geophys. Res. Lett.* **46**, 13281–13289 (2019).
28. Fu, Y. et al. Characteristics of seasonal scale convective and stratiform precipitation in Asia based on measurements by TRMM precipitation radar (in Chinese). *Acta Meteorol. Sin.* **66**, 730–746 (2008).
29. Fu, Y., Liu, P., Lin, J. & Heng, Z. Analysis on frequency of convective storm rain in rainy season over southern China based on measurements by TRMM precipitation radar (in Chinese). *Torrential Rain Disasters* **30**, 1–5 (2011).
30. Fu, Y. et al. Climatic characteristics of the storm top altitude for the convective and stratiform precipitation in summer Asia based on measurements of the TRMM precipitation radar (in Chinese). *Acta Meteorol. Sin.* **70**, 436–451 (2012).
31. Fu, Y., Pan, X., Liu, G., Li, R. & Zhong, L. Characteristics of precipitation based on cloud brightness temperatures and storm tops in summer over the Tibetan Plateau (in Chinese). *Chin. J. Atmos. Sci.* **40**, 102–120 (2016).
32. Fu, Y. et al. Precipitation characteristics over the steep slope of the Himalayas observed by TRMM PR and VIRS. *Clim. Dyn.* **51**, 1971–1989 (2018).
33. Zhang, A. & Fu, Y. Life cycle effects on the vertical structure of precipitation in East China measured by Himawari-8 and GPM DPR. *Mon. Weather Rev.* **146**, 2183–2199 (2018).
34. Randles, C. et al. The MERRA-2 aerosol reanalysis, 1980 onward. Part I: system description and data assimilation evaluation. *J. Clim.* **30**, 6823–6850 (2017).
35. Sun, N., Chen, Y. L. & Fu, Y. F. Characteristics of temperature and humidity profiles in Eastern China and their impacts on radiation budget (in Chinese). *Acta Meteorol. Sin.* **77**, 563–578 (2019).
36. Guo, J., Luo, Y., Yang, J., Furtado, K. & Lei, H. Effects of anthropogenic and sea salt aerosols on a heavy rainfall event during the early-summer rainy season over coastal Southern China. *Atmos. Res.* **265**, 105923 (2022).
37. Zhao, C., Peng, D. & Duan, Y. The impact of sea-salt and nss-sulfate aerosols on cloud microproperties. *J. Appl. Meteorol. Sci.* **16**, 417–425 (2005).

ACKNOWLEDGEMENTS

This work was funded by the National Natural Science Foundation of China Project (Grant Numbers: 41830104, 91837310), the Second Tibetan Plateau Scientific Expedition and Research (STAIRCASE) program (Grant Number 2019QZKK0104), and the Key Research and Development Projects in Anhui Province (Grant Number 201904a07020099).

AUTHOR CONTRIBUTIONS

N.S. and Y.F. framed up this study. All the authors discussed the concepts. N.S. conducted the data analyses. N.S. drafted the manuscript and all authors edited the manuscript.

COMPETING INTERESTS

The authors declare no competing interests.

ADDITIONAL INFORMATION

Supplementary information The online version contains supplementary material available at https://doi.org/10.1038/s41612-022-00284-0.

Correspondence and requests for materials should be addressed to Yunfei Fu.

Reprints and permission information is available at http://www.nature.com/reprints

Publisher's note Springer Nature remains neutral with regard to jurisdictional claims in published maps and institutional affiliations.